TRANSVERSE AND LONGITUDINAL MODES IN WAVEGUIDE-COUPLED RESONATORS

William D. Hunt, Tom Cameron,[1] John C. B. Saw,[1] Yoonkee Kim, and Mark S. Suthers[1], School of Electrical Engineering, The Microelectronics Research Center, Georgia Institute of Technology, Atlanta, Georgia 30332
[1]Bell Northern Research Ltd., P.O. Box 3511 Station C, Ottawa, Ontario, Canada K1Y 4H7

ABSTRACT: Surface acoustic wave (SAW) waveguide-coupled (WGC) resonators are of considerable interest for narrow-band filter applications though until recently there has been little published on the acoustic details of their operation. As in any resonator, one must fully understand its mode structure and herein we study the SAW mode profiles in these devices. Transverse and longitudinal mode profiles in the resonant cavity of the device were measured at various frequencies of interest using a knife-edge laser probe. In addition we predict the mode profiles for the device structure by two independent methods. One is a stack-matrix approach adapted from integrated optics and the other is a conventional analytical eigenmode analysis of the Helmholtz equation. Both modelling techniques are in good agreement with the measured results.

I. INTRODUCTION

Surface acoustic wave (SAW) waveguide-coupled (WGC) resonators, as shown in Figure 1, are a class of devices which are proving to be quite useful in narrow band filtering applications.

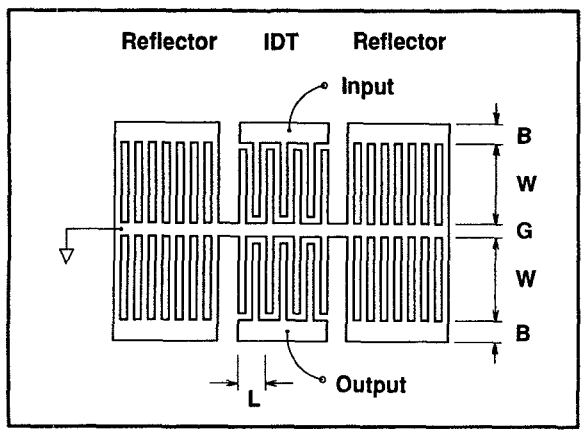

Figure 1 Schematic layout for a waveguide-coupled resonator

Though these devices were proposed quite some time ago[1] there has since been only a few papers published on these devices. Tanaka, et al.,[2] have published the most comprehensive analysis of the WGC resonator to date, using an analytical modal analysis to predict the resonant frequencies of the device and the frequencies of the spurious modes. Their work provides a relatively comprehensive introduction to the device, giving the reader an intuitive feel for the relationship between the transducer overlap width, W, coupling gap, G, and the mode structure. However, they have not published an accurate means of predicting the frequencies of the resonant and spurious modes.

Gopani and Horine[3] more recently have presented the frequency characteristics of various WGC resonators they have fabricated. Their results indicate they have been able to reduce the level of the spurious modes considerably but they provide no insights into their methods for achieving this. There were several papers on WGC resonator filters presented at the 1992 IEEE Ultrasonics Symposium clearly indicating a considerable industrial and university effort is underway.

In the process of designing a WGC resonator for a specific application one is typically concerned about the center frequency and bandwidth of the device as well as the spurious modes of the device. These devices are quite complicated and a detailed understanding must employ both the coupling of modes (COM) analysis[4,5] and the treatment of the device as a SAW structure supporting a collection of guided modes. Both of these analyses are key but in this paper we will focus principally on the SAW waveguide and cavity aspects of the WGC resonator.

For this investigation a number of WGC resonator devices were designed and fabricated each with different values for W, G, and C. Numerous measurements were made to determine the relationship between device geometry and the device transfer function but herein we will only discuss the amplitude profiles of the SAW transverse and longitudinal modes which were measured using a knife-edge laser probe.[6] In general, our approach was to measure the transverse mode profiles at the resonant frequencies associated with peaks in the magnitude response of the transfer function of the WGC resonator.

In this paper we predict the transverse beam profiles by two distinctly different techniques. These methods yield the eigenmodes of the device structure and they compare favorably in shape with the mode profiles measured using the laser probe and this corroboration between theory and experiment represents a considerable increase in the collective understanding of WGC resonators.

II. DEVICE DESCRIPTION

Our design for the WGC resonator is shown schematically in Figure 1. The device can be thought of as two one port SAW resonators coupled acoustically by

VV

3CH3277-1/93/0000-1509$01.00 © 1993 IEEE

the overlap of their respective eigenmodes.

In Figure 2 we present the transfer function for a WGC resonator. The passband response as well as the spurious response are set by the modes within the device. Peaks in the frequency response occur near frequencies which support both longitudinal and transverse modes. As will be shown , the lower edge of the passband, f_{s1}, in Figure 2 is a symmetric mode and the upper edge of the passband, f_{a1}, is an antisymmetric mode. The nearby spurious mode, f_{s2}, is a higher order antisymmetric mode. The synthesis task which presents itself to the designer is to control the strength and location of these modes through design. The present work is a step towards this goal in as much as it provides some of the tools necessary to effectively perform this synthesis.

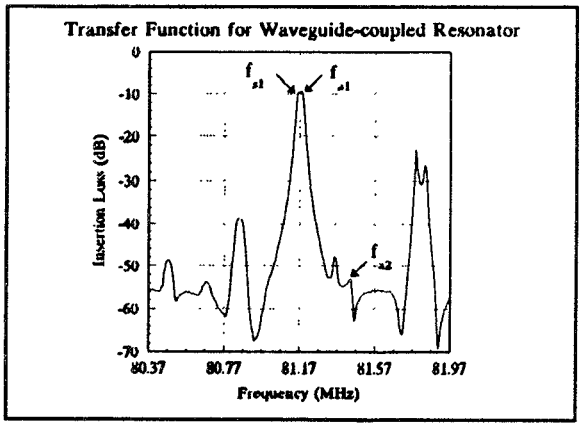

Figure 2 Transfer function of a WGC resonator

III. METHODS FOR EIGENMODE CALCULATIONS

The transverse mode profiles were predicted using two independent methods. The analytical method is the traditional approach of solving the Helmholtz equation in the slow and fast regions and matching the solutions at the boundaries. The stack matrix method has been adapted from integrated optics and is extremely versatile. With the stack matrix one can analyze a waveguide or mutlichannel waveguide with an arbitrary number of velocity sections. The results from these techniques are compared with experimental results in the next section.

For the stack matrix approach we will use the Helmholtz equation for the scalar potential, ϕ_i , in sectio i, the solution of which is

$$\phi_i(x) = A_i e^{-jk_i x} + B_i e^{jk_i x}$$

where β is the longitudinal propagation constant, ω is the angular frequency, and V_i is the SAW velocity in the i-th section and $k_i = (\frac{\omega^2}{V_i^2} - \beta^2)^{1/2}$. We have made the conventional assumption that the z-dependence is $e^{-j\beta z}$ and the time dependence is $e^{j\omega t}$. The boundary conditions at the interface between the i-th and the (i+1)-th are that the displacement and the stress are continuous.

Stack matrix theory begins by defining the continuous components used in the boundary condition to be the field variables, U and W, as follows

$$U_i = \phi_i(x) = A_i e^{-jk_i x} + B_i e^{jk_i x}$$
$$W_i = C_i \phi_i'(x) = jk_i C_i \left(-A_i e^{-jk_i x} + B_i e^{jk_i x}\right) \quad (1)$$

where C_i is the effective stiffness constant for the i-th region.

After some algebraic manipulations, one can obtain a simple relationship between two adjacent field variables as follows

$$\begin{bmatrix} U_{i-1} \\ W_{i-1} \end{bmatrix} = \begin{bmatrix} \cos k_i w_i & -\frac{1}{C_i k_i}\sin k_i w_i \\ C_i k_i \sin k_i w_i & \cos k_i w_i \end{bmatrix} \begin{bmatrix} U_i \\ W_i \end{bmatrix} = M_i \begin{bmatrix} U_i \\ W_i \end{bmatrix} \quad (2)$$

where w_i is the width of the i-th section and M_i is the *characteristic matrix* of the section. The repeated application of the boundary conditions at each interface is accomplished by the concatenation of each M_i. Therefore, the *characteristic matrix* of the stack, M, which includes the entire structure is given by

$$\begin{bmatrix} U_0 \\ W_0 \end{bmatrix} = M_1 M_2 \cdots M_N \begin{bmatrix} U_N \\ V_N \end{bmatrix} = M \begin{bmatrix} U_N \\ W_N \end{bmatrix} = \begin{bmatrix} m_{11} & m_{12} \\ m_{21} & m_{22} \end{bmatrix} \begin{bmatrix} U_N \\ W_N \end{bmatrix} \quad (3)$$

For the guided wave solutions, ϕ should be evanescent at both ends, i.e. for both $i = 0$ and $i = N$ sections. This guided condition is satisfied by a pure imaginary value of k_i at both sides and $B_0 = A_{N+1} = 0$. This will lead to the matrix equation

$$\begin{bmatrix} 1 & -m_{11} + C_{N+1}\gamma_{N+1} m_{12} \\ C_0\gamma_0 & -m_{21} + C_{N+1}\gamma_{N+1} m_{22} \end{bmatrix} \begin{bmatrix} A_0 \\ B_{N+1} \end{bmatrix} = \begin{bmatrix} 0 \\ 0 \end{bmatrix} \quad (4)$$

where $\gamma_0 = j(\beta^2 - \frac{\omega^2}{V_0^2})^{1/2}$, $\gamma_{N+1} = j(\beta^2 - \frac{\omega^2}{V_{N+1}^2})^{1/2}$

In order to obtain a non-trivial solution, the determinant of the matrix must be set to zero thus yielding the dispersion relation for the waveguide. For the general multichannel waveguide structures, a numerical method is necessary to solve the matrix equation.

IV. MEASUREMENTS AND RESULTS

In this section we will present experimental measurements of a WGC resonator on STX-Quartz and compare these results with theoretical predictions based on the methods referenced in Section III. Though numerous devices were fabricated and tested we will present only the results from one of these which had strong spurious modes. While this device would not be good for a system application, it was an ideal device for our mode profile measurements. The results we present, however, were consistently demonstrated for various devices.

The device was mounted on the computer-controlled translation stage of our knife-edge laser probe and leveled. The details of operation of this apparatus has been described previously[6] and will not be repeated here. It is sufficient to say that the laser probe allows us to measure the magnitude and phase of a Rayleigh wave at various locations throughout the device. For these experiments the laser spot at the surface of the device was approximately 4μm in diameter and the signal to noise ratio of the measurements was around 60 dB. The successful operation of the laser probe requires that the location of the scan on the surface of the device have a reasonable reflectance and so the measurements were made with the laser spot on the aluminum electrodes of the IDT and on the bus bar rather than on unmetallized Quartz. From the device transfer function shown in Figure 2 we select the frequencies at which we wish to make transverse laser probe scans. For example, if we wish to measure the mode profile for the first symmetric mode we set the SAW drive for the device at the first symmetric mode frequency, f_{s1} , and scan transverse to the direction of SAW propagation. Similarly we can select the frequencies associated with any of the spurious modes which appear in the transfer function and measure the associated mode profiles. Longitudinal scans were made parallel to the direction of SAW propagation with the spot on the outside bus bar as close as possible to the electrode overlap region.

For the mode profile data we present, the origin of the coordinate system was set such that x = 0 (the transverse dimension) was on the central bus bar which connects the ground electrodes for both tracks and y=0 (the longitudinal dimension) was at the midpoint between the reflectors. The transverse scans were all taken at the center of the cavity. The symmetric modes were obtained when the two tracks were driven by the same source. The antisymmetric modes were obtained with a balun drive, i.e., the two tracks were driven 180° out of phase. In Figure 3 we show the measured and predicted normalized magnitudes of the first symmetric mode. The magnitude is expressed in arbitrary units (A.U.). Both theoretical approaches predict the same shape with the profile reaching peaks in the middle of the tracks and reaching a local minimum on the grounded bus bar between. The phase data also compared very well with the theoretical predictions but will not be presented here due to a lack of space.

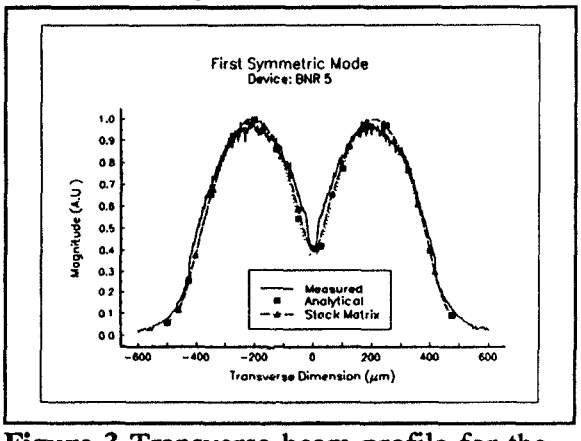

Figure 3 Transverse beam profile for the first symmetric mode

In Figure 4 we present the magnitude for the mode profile of the first antisymmetric mode. Again there is good comparison between theory and experiment. The profile is, of course, quite similar to that for the first symmetric mode with the exception that the profile goes to zero at the central bus bar for the antisymmetric mode.

In Figure 5 we present the normalized magnitude for the first antisymmetric mode. Again there is good agreement between experiment and the two theoretical predictions though the agreement is not as precise as for the first symmetric and antisymmmetric modes. This is in part due to the lower signal strength associated with

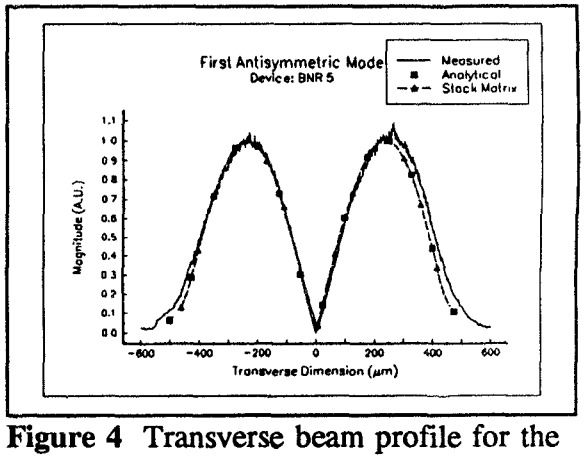

Figure 4 Transverse beam profile for the first antisymmetric mode

the second antisymmetric mode and the fact that what we measure is a superposition of the second antisymmetric and first antisymmetric modes.

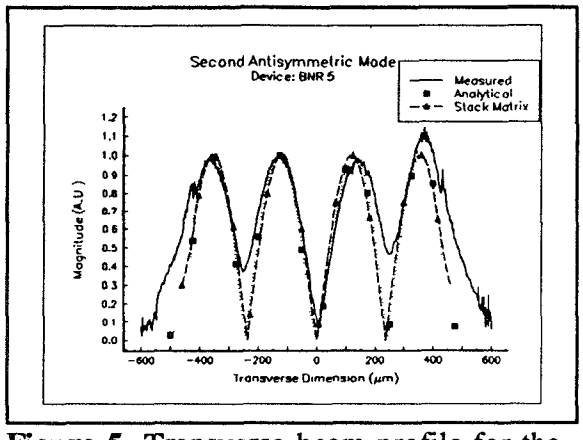

Figure 5 Transverse beam profile for the second antisymmetric mode

In Figure 6 we present the longitudinal scan for the second symmetric mode. This shape was very similar to what was measured at f_{s1}, , f_{a1}, and f_{a2}, which supports Tanaka[2] conjecture that these transverse modes are supported by a fundamental longitudinal mode.

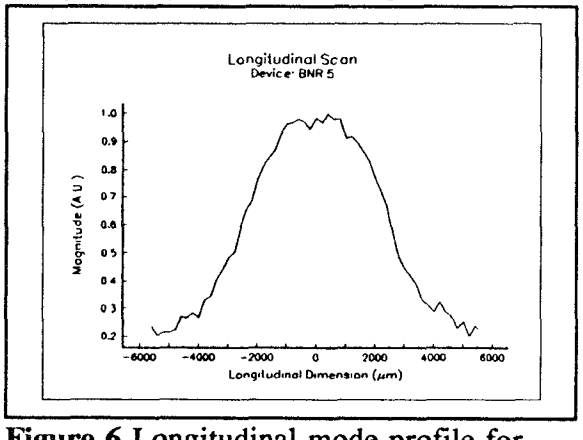

Figure 6 Longitudinal mode profile for second symmetric mode

V. SUMMARY AND CONCLUSIONS

In this paper we have presented both experimental and theoretical work on the mode profiles in WGC resonators. The two independent methods for predicting the mode profiles are reasonably accurate though the stack matrix theory method is the most versatile of the two. This paper represents, to the best of our knowledge, the first use of stack matrix theory to predict mode profiles in SAW structures. The versatility and accuracy of this technique makes it useful for the calculation of mode profiles in complicated, multichannel SAW and ACT devices.

ACKNOWLEDGEMENTS

This work has been supported by Bell Northern Research Ltd. (BNR), the National Science Foundation through a Presidential Young Investigator award and by NASA under grant #NAGW-2753. The assistance of these organizations is gratefully acknowledged. We also wish to thank Grantley Este of BNR for many helpful discussions with regard to the fabrication of SAW devices, Conrad Gratton of BNR for initial testing and packaging of the devices and Robert Schaefer of Georgia Tech for assistance in the laser probe measurements and data analysis.

REFERENCES

[1]Yamada, A. and Shimizu, H., *Paper of the Technical Group on Ultrasonics, IECE, Japan,* VS77-33, p. 29, 1977.

[2]Tanaka, M., Morita, T., Ono, K. and Nakazawa, Y., *38th Annual Frequency Control Symposium,* pp. 286-293. 1984.

[3]Gopani, S. and Horine, B. A., *Proceedings of the 1990 IEEE Ultrasonics Symposium,* pp. 1-5, 1990.

[4]Kogelnik, H. and Shank, C.V., *Journal of Applied Physics,* vol. 43, pp. 2327-2335, May 1972.

[5]Haus, H.A. and Wright, P.V., *Proceedings of the 1980 IEEE Ultrasonics Symposium,* IEEE Cat. No. 80CH1602-2, Vol. 1, pp. 277-281, 1980.

[6]Miller, R.L., Ph.D. dissertation, University of Illinois, Urbana, Illinois, 1987.